Macromolecules

ARTICLE

pubs.acs.org/Macromolecules

Microgel-Reinforced Hydrogel Films with High Mechanical Strength and Their Visible Mesoscale Fracture Structure

Jian Hu,[†] Kenta Hiwatashi,[†] Takayuki Kurokawa,[‡,§] Song Miao Liang,[‡] Zi Liang Wu,[†] and Jian Ping Gong*[,‡]

[†]Graduate School of Science, Hokkaido University, Sapporo 060-0810, Japan

[‡]Faculty of Advanced Life Science, Hokkaido University, Sapporo 060-0810, Japan

[§]Creative Research Initiative Sousei, Hokkaido University, Sapporo 001-0021, Japan

ABSTRACT: The poor mechanical properties remain the largest barrier to traditional synthetic hydrogels for extensive practical applications, such as tissue scaffolds. In this work, we have synthesized the hydrogel films in the presence of microgel precursors of various chemical species with different charges. The hydrogels fabricated have a novel two-phase composite structure, where the continuous phase is a loosely cross-linked polyacrylamide (PAAm) matrix and the disperse phase is virtually double-network (DN) microgels. Named as microgel-reinforced (MR) hydrogels, they exhibited dramatic enhancement in mechanical strength and toughness, in comparison to the hydrogels with no microgels. MR hydrogels showed the comparable mechanical properties with the conventional bicontinuous DN hydrogels. By visualizing the embedded microgels before, during, and after the elongation, mesoscale fractures of the microgels phase were confirmed, which should effectively blunt the crack and enhance the fracture propagation resistance. Therefore, we conclude that the essential reinforcement principle of MR gels roots in the sacrificial bonds effect contributed by the microgels. This work provides a novel universal pathway to synthesize hydrogel thin films with high strength and toughness from various microgels and may open a new avenue for the application of hydrogels in various fields, such as fast responsive actuators, fuel cell films, wound dressings, etc.

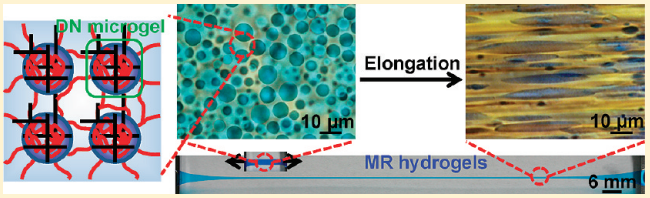

INTRODUCTION

Hydrogels are polymeric materials that maintain a distinct three-dimensional structure when swollen in water. Traditional synthetic hydrogels show the low mechanical strength due to the heterogeneous network structure; therefore, studies on hydrogels had been always focused on the applications in responsiveness, such as drug delivery systems, sensors, and smart "on−off" valves.[1] Calvert suggested that if we can develop hydrogels that combine high mechanical strength with responsiveness and fast diffusion, we can envision new families of soft biomimetic machines.[2] To date, many attempts have been made to fabricate hydrogels with various optimized network structures to reinforce the mechanical strength, such as DN hydrogels,[3] inverted DN hydrogels,[4−6] slide-ring hydrogels,[7] nanocomposite hydrogels,[8−11] tetra-PEG hydrogels,[12] dendrimer/clay composite hydrogels,[13] triblock copolymer hydrogels,[14,15] cyclic hydrogels,[16] hydrogen-bonding hydrogels,[17] and, most recently, hydrophobic lamellar bilayer composite hydrogels.[18]

Inspired by carbon black (CB) reinforced rubbers, introduction of a hard phase into hydrogels seems to be a feasible way to increase the mechanical strength. However, in most particle-containing hydrogel systems, particles are impregnated into hydrogels to improve the responsive properties to various external stimuli, without obvious improvement in mechanical strength.[19−21] The poly(dimethylacrylamide)/silica hybrid hydrogels indicate that incorporation of silica nanoparticles (radius = 9.3 nm) in the hydrogel increases the compression strength (modulus = 0.18 MPa) and the fracture toughness (fracture energy = 80 J/m^2) of notched samples up to 1 order of magnitude, but they are still too brittle to perform the tensile test.[22] More attention has been on macromolecular microsphere composite (MMC) hydrogels, in which peroxidized microspheres (diameter ca. 100 nm) act as both initiator and cross-linker, grafting poly(acrylic acid) chains on the surface of microspheres.[23] MMC hydrogels exhibit good compressive performance, but no tensile and tearing properties that truly reflect the resistance against crack propagation have been reported, probably also due to the brittleness of the MMC gels.

The reinforcement mechanism of DN gels has been extensively studied, and it has been elucidated that the rigid and brittle polyelectrolyte network serves as sacrificial bonds to increase the resistance against the crack propagation by forming a large damage zone at the crack tip.[24] From this DN gel mechanism, we assume that introduction of any effective sacrificial bonds will reinforce the material. On the basis of this assumption, we are attempting to induce various kinds of sacrificial bonds into the hydrogel. One successful approach was recently found to fabricate strong DN gels from poly(2-acrylamido-2-methylpropanesulfonic acid) (PAMPS) powder precursors that were obtained by grinding the dried bulk PAMPS hydrogels. The so-called P-DN hydrogels containing PAMPS particles in the PAAm matrix exhibited comparable strength and toughness with those of standard DN gels.[25] The result suggests that the polyelectrolyte

Received: June 2, 2011
Revised: August 19, 2011
Published: September 08, 2011

Scheme 1. Preparation Procedure of Quasi-Monodisperse Microgels by SPG Membrane Emulsification and UV Polymerization

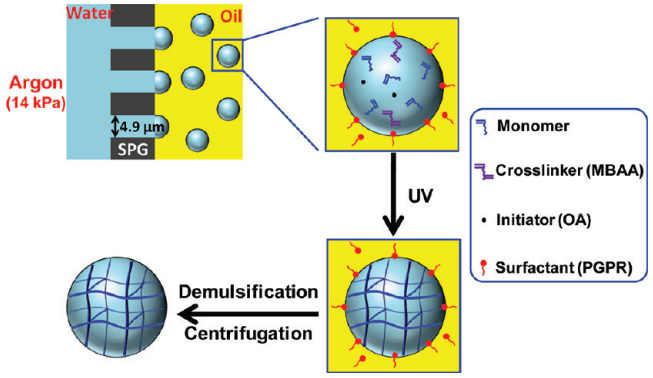

particles may also serve as the sacrificial bonds to reinforce the gel. The P-DN hydrogels from grinded PAMPS particles, however, possess a rough appearance and poor reproducibility. It is also unpromising for the study of the fracture process due to the irregular shape and a wide size distribution. Consequently, in this work, we have fabricated tough hydrogel films with a two-phase composite structure by embedding densely cross-linked quasi-monodisperse microgels (diameter ca. 5 μm) of various chemical species with different charges into a sparsely cross-linked neutral PAAm matrix. These microgel-reinforced hydrogels, named as MR hydrogels, show excellent mechanical strength and toughness. In addition, these MR hydrogels have the great advantage on the study of the fracture mechanism according to the visible deformation and the mesoscale fracture of embedded microgels by an optical microscope.

EXPERIMENTAL SECTION

Materials. 2-Acrylamido-2-methylpropanesulfonic sodium (NaAMPS) (Tokyo Kasei Co., Ltd.), *N,N*-dimethylamino propylacrylamide methyl chloride quarternary for DMAPAA-Q (Kohjin Co., Ltd.), *N,N*-dimethylamino ethylacrylate methyl chloride quarternary for DMAEA-Q (Kohjin Co., Ltd.), and sodium *p*-styrenesulfonate (NaSS) (Tokyo Kasei Co., Ltd.) as monomers were used as received. *N,N′*-Methylenebis(acrylamide) (MBAA) (Tokyo Kasei Co., Ltd.) as cross-linking agent was recrystallized from ethanol. Acrylamide (AAm) (Junsei Chemical Co., Ltd.) was recrystallized from chloroform. 2-Oxoglutaric acid (OA) (Wako Pure Chemical Industries, Ltd.) as UV initiator was used as received. Polyglycerol polyricinoleate (PGPR) (Danisco Co., Ltd.) as surfactant and kerosene (Wako Pure Chemical Industries, Ltd.) were used as received. Alcian Blue and Allura Red (Wako Pure Chemical Industries, Ltd.) as dyes were used as received. Milli-Q (18.3 MΩ) water was used in all experiments.

Preparation and Characterization of Microgels.[26] As shown in Scheme 1, W/O emulsion was prepared by high-speed mini kit equipped with hydrophobic SPG (Shirasu Porous Glass) membrane (SPG Technology Co., Ltd.). The disperse phase was an aqueous solution of 1 M NaAMPS containing 4 mol % cross-linking agent MBAA and 0.1 mol % UV initiator OA, with respect to NaAMPS monomer. The disperse phase, stored in a pressure-tight vessel, was pressed into the continuous phase, kerosene containing 1 wt % surfactant PGPR, through the hydrophobic SPG membrane (pore diameter = 4.9 μm) under argon transmembrane pressure of 14 kPa. After bubbling by argon for 1 h, the W/O emulsion was polymerized for 8 h by a 365 nm UV lamp under an argon atmosphere. The poly(2-acrylamido-2-methylpropanesulfonic sodium) (PNaAMPS) microgels were precipitated with acetone from the emulsion and in deionized water and then separated by centrifugation at 10^4 rpm (3 times). After freeze-drying, the dried PNaAMPS microgels were obtained as fine powders. The PNaAMPS microgels were swollen in water until equilibrium was reached, and optical images were captured by a differential interference contrast microscope (DIC; Olympus BX50). The size distribution of the microgels was determined by measuring the diameters of 300 microgels in the captured DIC images with an analytic software, Image-Pro Plus. To evaluate the dispersity of the microgels quantitatively, the coefficient of variation is defined as $CV = (\sigma/D_m) \times 100\%$, where σ is the standard deviation of microgel diameter and D_m is the number-average mean microgel diameter. The resulting anionic PNaAMPS microgels (−) were ca. 5 μm in D_m and 28.6% in CV, which could be considered as quasi-monodisperse.[27]

Cationic *N,N*-dimethylamino propylacrylamide methyl chloride quarternary for DMAPAA-Q microgels (+), neutral polyacrylamide (PAAm) microgels (0), copolymer microgels (±) of cationic poly(N,N-dimethylamino ethylacrylate methyl chloride quarternary for DMAEA-Q) and anionic poly(sodium *p*-styrenesulfonate) (PNaSS) (molar ratio: 1:1) were prepared with the same preparation method as above.

Preparation and Characterization of MR Hydrogels. As shown in Scheme 2, 0.07 or 0.075 g of dried microgel powders was immersed in 1 mL of aqueous solution containing 2 M AAm, 0.01 mol % MBAA, 0.01 mol % OA, and 4 M sodium chloride (NaCl). The NaCl was used to control the solution at suitable operating viscosity. After equilibrium swelling, the pastelike solution was poured into the mold consisting of two parallel glass plates and 100 μm silicone spacer and then polymerized under an argon atmosphere with UV lamp for 8 h. The as-prepared hydrogels were desalinated completely in deionized water and were denoted as sMR hydrogels for its single PAAm network structure. Then the sMR gels were swelled in an aqueous solution of 4 M AAm containing 0.01 mol % MBAA and 0.01 mol % OA once again. After equilibrium swelling, the sMR gels were covered by two parallel glass plates and then irradiated under an argon atmosphere with UV lamp for 8 h to polymerize AAm again. Finally, the gels were swelled in deionized water to remove the residual monomers, and the tough MR gels with two interpenetrated PAAm network were obtained. Cationic−anionic mixed MR gel (+/−) was prepared from the mixture of PDMAPAA-Q microgels and PNaAMPS microgels (molar ratio: 1:1). In this paper, MR hydrogels were coded as sMR(x)y and MR(x)y, where "s" stands for MR hydrogels with a single PAAm network. "x" indicates the charged nature of microgels used, and "y" is the concentration of dried microgels added to AAm solution in g/mL. As a reference, a pure PAAm gel was also prepared by the two-step sequential polymerization without adding microgels. In addition, a double-network (DN) hydrogel film was prepared as the method described in our previous work.[28]

The apparent absorbance A of the hydrogels was measured at a wavelength of 550 nm and room temperature by a model 680XR plate reader (Bio-Rad). A was the average of five measurements at different spots on one sample. In order to compare the transparency between samples of different thickness, we calculated the turbidity coefficient t of all the samples from the equation described by $t = A/w$ assuming t is uniform for the sample, where t is the intrinsic parameter related to the absorption coefficient and the scattering coefficient and w is the thickness of the samples measured by an optical microscope.

The equilibrium swelling ratio q_w is defined as $q_w = W_{eq}/W_{dry}$, where W_{eq} and W_{dry} are the weight of hydrogels in the fully water-swollen state and dry state, respectively.

The tensile test was performed with a commercial test machine (Tensilon RTC-1150A, Orientec Co.). The fully swelled samples were cut into a dumbbell shape as standardized JIS-K6251-7 sizes (length 35 mm, width 2 mm, gauge length 12 mm) with a gel cutting machine (Dumbbell Co., Ltd.). Both ends of the dumbbell-shaped samples were clamped and stretched at a constant velocity of 100 mm/min. The fracture stress σ_b and fracture strain ε_b were the values at breaking point. Tensile modulus

dx.doi.org/10.1021/ma2016248 |*Macromolecules* 2011, 44, 7775–7781

Scheme 2. Procedure for Preparing Microgel-Reinforced (MR) Hydrogels from Various Microgel Precursors[a]

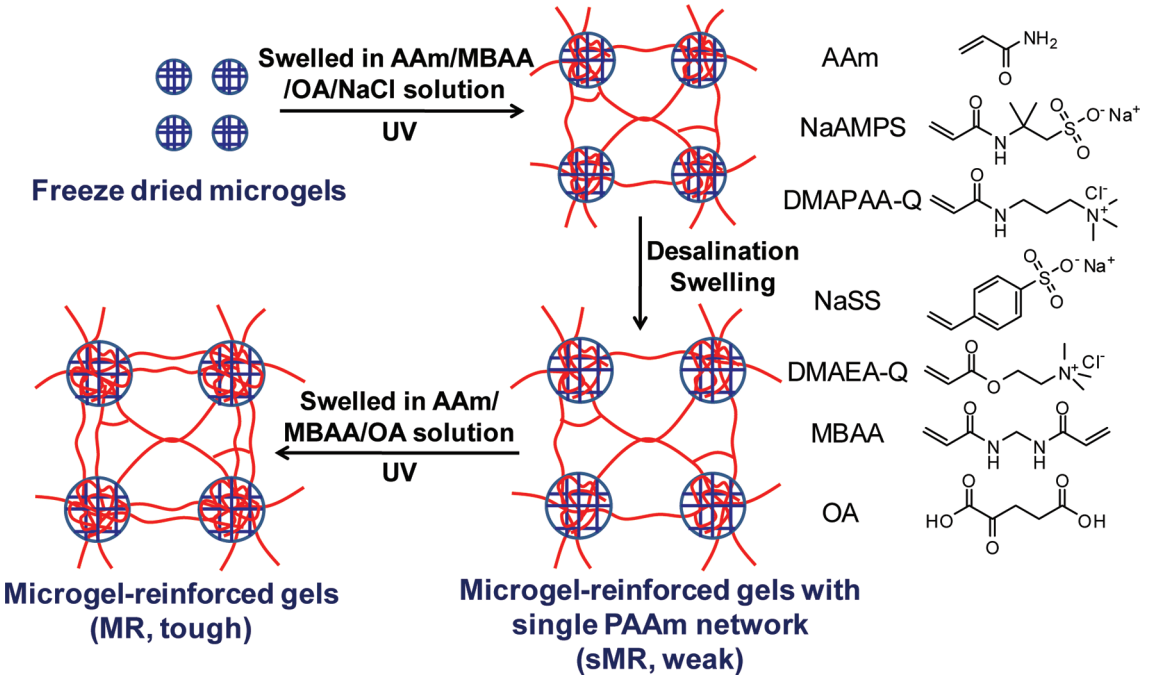

[a] Neutral PAAm microgel (0), anionic PNaAMPS microgel (−), cationic PDMAPAA-Q microgel (+), P(DMAEA-Q-*co*-NaSS) microgel (±), and the mixture of PNaAMPS microgel and PDMAPAA-Q microgel (+/−) were used.

Scheme 3. Dyeing Principle of Polyelectrolyte Microgels Based on Electrostatic Attraction

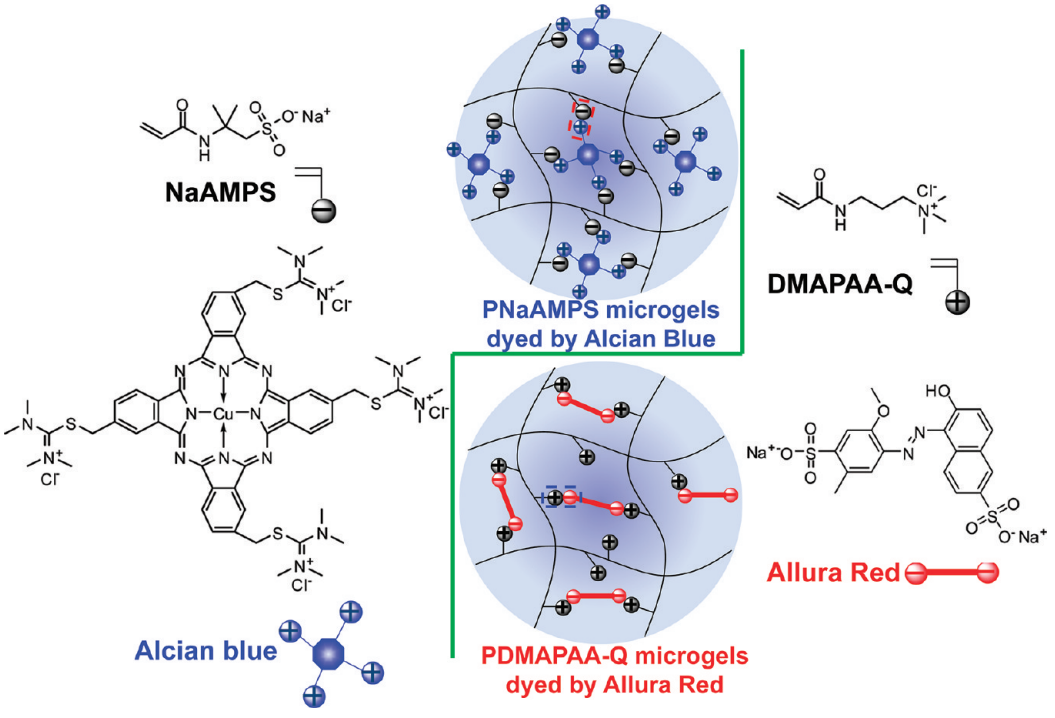

E was determined from the slope within the initial linear region (less than 10% strain) of the stress−strain curves. The dissipated energy at fracture W_b was calculated as the area under the stress−strain curve.

The tear test was performed in Mode III (Tearing mode)[29] with the commercial test machine. The fully swelled samples were cut into a trousers shape as standardized JIS-K6252 1/2 sizes (length 50 mm, width 7.5 mm, the initial notch 20 mm) with the gel cutting machine. The two arms of the test samples were clamped, and one arm was pulled upward at a constant velocity of 100 mm/min, while the other arm was fixed. The tearing energy, *T*, is defined as the work required to tear a unit

dx.doi.org/10.1021/ma2016248 |*Macromolecules* 2011, 44, 7775–7781

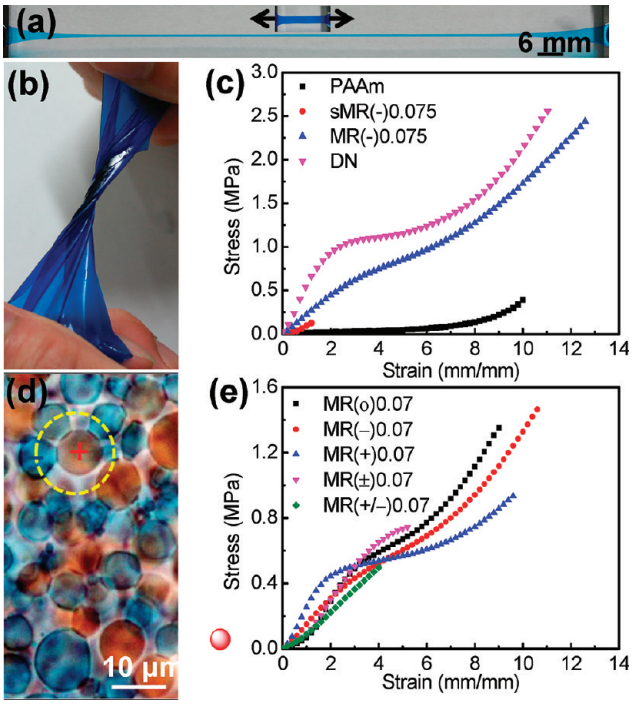

Figure 1. MR(−)0.07 gel film, dyed by Alcian Blue, subject to high elongation from the free-standing state to the stretching state of strain = 11 mm/mm (a) and torsion (b). (c) Comparison of tensile stress−strain curves of PAAm, sMR(−)0.075, MR(−)0.075, and DN gels. (d) Optical microscopy image of MR(+/−)0.07 gel dyed by Alcian Blue and Allura Red, minus symbol, plus symbol and yellow dashed line indicate anionic PNaAMPS microgel (−), cationic PDMAPAA-Q microgel (+), and the interaction between them, respectively. (e) Comparison of tensile stress−strain curves of various MR gels based on five sorts of microgels.

area, calculated by $T = 2F_{ave}/w$,[30] where F_{ave} is the average force of peak values during steady-state tear and w is the thickness of the test samples. It should be noted that the T is defined as 2 times the fracture energy G used in our previous papers.[31,32] The latter is defined as the energy to create a unit area of fracture surface.

Selective Dyeing of Polyelectrolyte MR Gels. Scheme 3 shows the selective dyeing of the polyelectrolyte microgels: MR(−) gel was immersed in 3 vol % acetic acid aqueous solution of 1 wt % Alcian Blue for 15 min and then washed in deionized water. MR(+/−) gel was dyed by double staining, described as two-step subsequent staining of 3 vol % acetic acid aqueous solution of 1 wt % Alcian Blue for 15 min and 0.1 wt % Allura Red aqueous solution for 15 min, respectively, and then washed in deionized water.

RESULTS AND DISCUSSION

As shown in Figure 1, the MR(−)0.07 gel film was capable of subjecting to dramatic elongation (Figure 1a) and torsion (Figure 1b), exhibiting extraordinary ductility and flexibility. Figure 1c shows the tensile stress−strain curves of sMR(−)0.075 and MR(−)0.075 gels. The behavior of the PAAm gel, prepared by the same two-step sequential network formation of PAAm without adding microgels, was used for comparison (shown in Figure 1c). The PAAm gel was very soft and ductile (modulus E, fracture stress σ_b, and fracture strain ε_b were 0.03 MPa, 0.4 MPa, and 1000%, respectively). In contrast, MR(−)0.075 gel exhibited high E, σ_b, and ε_b up to 0.22 MPa, 2.5 MPa, and 1300%, respectively. The reinforcement efficiency (the ratio of σ_b of MR(−)0.075 to that of the PAAm gel) reached up to 6 times, which showed the same order of magnitude as CB-reinforced vulcanizates.[33] On one hand, the increase in E is expected due to the addition of the relatively rigid microgels. (The E of microgels interpenetrated by PAAm networks was 0.34 MPa estimated from bulk gels with the same composition.) On the other hand, the increased E is also a result from the introduction of topologically constrained chain entanglements between penetrating chains of the matrix and those of the microgels. So the embedded microgels play a role as multifunctional physical cross-linking points, which effectively transfer energy across the matrix/microgel interface. The problem resides in the ability of the microgels to permit a much increased elongation at break, which perhaps stems from the abundant coiled PAAm chains stored compactly in the highly cross-linked microgels. However, sMR(−)0.075 gel was very brittle, broke at the strain of 100%, which indicates that the molar ratio of the PAAm matrix to microgels is vital to fabricate MR hydrogels with high mechanical strength. To make a comparison between DN gels and MR gels, the tensile result of the DN gel film is also shown in Figure 1c. Comparing with the DN gel, MR(−)0.075 gel showed a comparable σ_b and a slightly higher ε_b. However, MR(−)0.075 gel showed a much lower initial modulus E than that of the DN gel, which is apparently due to the discontinuous distribution of the microgels.

As shown in Figure 1e, this microgel-reinforced effect was observed for other microgels studied, where MR hydrogels were fabricated at a lower microgel concentration of 0.07 g/mL. The samples from neutral PAAm microgel (MR(0)0.07), anionic PNaAMPS microgel (MR(−)0.07), and cationic PDMAPAA-Q microgel (MR(+)0.07) showed the similar fracture strain while MR(−)0.07 gel exhibited the highest fracture stress. A well-defined yielding behavior was observed for MR(+)0.07 gel. These variations should be related to the difference in the swelling ratio and the cross-linking density of microgels, which is due to the difference in reaction activity with cross-linker.

On the other hand, samples from P(DMAEA-Q-*co*-NaSS) copolymer microgel (MR(±)0.07) and from the mixture of cationic PDMAPAA-Q microgel and anionic PNaAMPS microgel (MR(+/−)0.07) exhibited a relatively brittle fracture behavior; especially, the MR(+/−)0.07 gel showed the brittle fracture behavior without yielding point. Figure 1d shows the optical microscopy image of MR(+/−)0.07 gel swelled in water, where the anionic PNaAMPS microgels (blue) and the cationic PDMAPAA-Q microgels (red) were dyed by double staining. In this picture, the intense interaction between the anionic microgels and the cationic microgels was observed clearly, confirming the existence of a considerable amount of mesoscale aggregates, and the anionic microgels showed a larger deformation, indicating the lower modulus than the cationic microgels. The strong aggregation of microgels leads to the stress concentration and fast development of defects to cracks in MR(+/−)0.07 gel, and thus, the PAAm matrix phase may fracture ahead of the microgel phase.

The specific characteristics of PAAm and various MR and DN hydrogels are summarized in Table 1. The thickness of all the gels was prepared at 200−300 μm in order to facilitate the visualization of the incorporated microgels by microscope. The PAAm gel and the DN gel showed a low turbidity t of 0.10 and 0.09 mm^{-1} (corresponding to a transmittance of 93% and 94%, respectively, for samples of 300 μm thick) and could be considered as perfectly transparent. All the MR hydrogels showed a notable increase in t, which stemmed from the scattering loss in the interface of the embedded microgels. The increased scattering

dx.doi.org/10.1021/ma2016248 |*Macromolecules* 2011, 44, 7775–7781

Table 1. Specific Characteristics of PAAm and Various MR and DN Gels

					tensile				tear
hydrogel category	sample	thickness w (μm)	turbidity t (mm^{-1})	swelling ratio q_w(g/g)	modulus E (MPa)	fracture stress σ_b (MPa)	fracture strain ε_b (mm/mm)	dissipated energy W_b (MJ/m^3)	tearing energy T (J/m^2)
neutral gel	PAAm	252	0.10	13.3	0.03	0.41	10.1	0.86	20
neutral MR gel	MR(0)0.07	292	0.17	11.1	0.05	1.37	9.1	5.78	704
anionic MR gels	sMR(−)0.07	166	0.19	21.5	0.01	0.06	1.6	0.03	56
	MR(−)0.07	277	0.56	7.7	0.13	1.47	10.6	7.12	500
	sMR(−)0.075	219	0.15	20.3	0.05	0.15	1.3	0.07	132
	MR(−)0.075	307	0.55	6.7	0.22	2.46	12.7	14.15	858
cationic MR gel	MR(+)0.07	259	1.41	7.4	0.15	0.94	9.7	5.34	442
cationic-*co*-anionic MR gel	MR(±)0.07	199	1.11	8.5	0.07	0.75	5.3	2.12	788
cationic−anionic mixed MR gel	MR(+/−)0.07	205	1.79	8.9	0.07	0.51	4.1	0.99	524
DN gel	DN	305	0.09	6.8	0.30	2.58	11.1	14.45	1228

loss was due to the increased concentration difference between PAAm chains existing in and around the microgels. Among them, MR(0)0.07 gel was an exception, with a low t of 0.17 mm^{-1}, corresponding to a transmittance of 89% for samples of 300 μm thick. Different from the polyelectrolyte microgels swelling to equilibrium in water spontaneously, the swelling of the neutral microgel was driven gradually by the osmotic pressure of the interpenetrated PAAm chains, which reduced the concentration difference of PAAm chains in and around the microgels. The homogeneity between the PAAm microgel and the PAAm matrix might be the other reason for the decreased t. It is interesting to compare MR(−)0.075 gel with the DN gel because of the similar swelling ratio q_w. MR(−)0.075 gel showed the comparable mechanical strength with the DN gel from the tensile and tearing results, which suggests that the internal fracture efficiency of the polyelectrolyte network of the microgels is higher than that in the bicontinuous DN gel, if considering the lower volume fraction of polyelectrolyte network in MR(−)0.075 gel. In comparison with the PAAm gel without microgels, MR hydrogels showed a decrease in the swelling ratio, indicating that microgels act as multifunctional physical cross-linking points.[22] From the results of tensile and tear test, there is a substantial improvement in the mechanical strength comparing various MR hydrogels with the PAAm gel. Comparing MR(−)0.075 gel with the PAAm gel, it increased 16 times in dissipated energy at fracture, W_b, and 43 times in tearing energy, T; these two parameters are commonly used to characterize the strength and toughness of materials. In fact, T of MR(−)0.075 gel came up to 858 J/m^2, which was close to the T of nonreinforced styrene−butadiene (SB) vulcanizate, that is, ca. 1000 J/m^2 tested at 50 °C by steady tearing.[30] Comparing with the pure PAAm gel, all the MR hydrogels gave the remarkable enhancements in mechanical strength and toughness, which indicates that the reinforcement phenomenon based on microgels incorporation has the universality. Therefore, it is attractive to pursue this kind of essential reinforcement mechanism in depth.

As shown in Scheme 2, MR gels are two-phase composites comprised of the PAAm matrix and microgels. The disperse phase incorporated in the final MR hydrogels has been considered as DN microgels. As has been clarified in our previous work,[34] the DN hydrogel becomes tough only when its structure

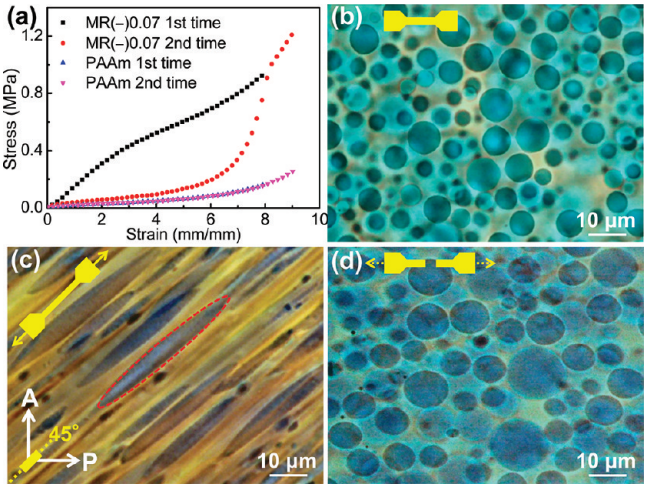

Figure 2. (a) Hysteresis in stress−strain curves of MR(−)0.07 gel and the PAAm gel. The first and the second elongation are stopped at the strain = 8 mm/mm and strain = 9 mm/mm, respectively. (b) Optical microscopy image of MR(−)0.07 gel film at the free-standing state. (c) Real-time tensile observation of MR(−)0.07 gel film at the strain of 4 mm/mm by a polarizing microscope, equipped with the crossed polarizers and the 530 nm tint plate. The sample was stretched 45° against the polarizers. The red dashed line indicates the deformed microgel. (d) Residual strain observation of reswollen MR(−)0.07 gel film after tensile fracture by an optical microscope. The elliptic shape of the micogels indicates the occurrence of the internal fracture after elongation. MR(−)0.07 gel film is dyed by Alcian Blue for (b−d).

satisfies the two conditions: (a) the first network is a densely cross-linked, rigid, and brittle polyelectrolyte network, whereas the second network is sparsely cross-linked, soft, and ductile, neutral network, and (b) the molar concentration of the second network is 20−30 times higher than that of the first network. Consequently, it is easy to understand why the low concentration of cross-linker MBAA for the first and second polymerization of PAAm is necessary to fabricate tough MR gels, satisfying condition (a). Also, sMR(−) gels were very weak due to the small molar ratio (4:1, calculated from volume change of microgels) of the PAAm matrix to the anionic PNaAMPS microgels, which does not satisfy the condition (b). By the second polymerization

dx.doi.org/10.1021/ma2016248 |*Macromolecules* 2011, 44, 7775–7781

of AAm solution, more PAAm chains were impregnated into the microgels to satisfy the condition (b). In other words, the first PAAm network aims to trap all the microgels, and the second PAAm network truly reinforces the MR hydrogels.

The reinforcement mechanism of DN gels with bicontinuous network structure has been elucidated that the rigid and brittle polyelectrolyte network serves as sacrificial bonds to increase the resistance dramatically against the crack propagation.[24] We assume that the high mechanical strength of MR gels root in the sacrificial bonds contributed by the DN microgels phase, similar to the fracture phenomenon occurred in DN bulk gels. This assumption is verified in Figure 2. MR(−)0.07 gel and the PAAm gel were first stretched to the strain the ε of 800% and then recovered to the origin, followed by the second elongation to the ε of 900% (Figure 2a). A prominent hysteresis was found for MR(−)0.07 gel, the same as DN gels,[35] but not for the PAAm gel. This result indicates that the irreversible structural change that is related to the rupture of covalent bonds occurred in the MR gel. In order to visualize this mesoscale fracture of MR(−)0.07 gel clearly, the anionic PNaAMPS microgels were dyed selectively by the tetravalent cationic Alcian Blue (Figure 2b). When MR(−)0.07 gel was elongated to the ε of 400%, the microgels deformed from sphere to prolate spheroid along with the stretching direction but showed a less ε than that of the bulk gel, corresponding to their higher modulus than the surrounding PAAm matrix phase (Figure 2c). The background color was attributed to the negative birefringence caused by the stretch orientation of the PAAm matrix, which changed with the degree of orientation.[36] Finally, the broken MR(−)0.07 gel was reswollen in deionized water (Figure 2d). Comparing Figure 2d with Figure 2b, by statistically measuring the size of 100 microgels in these images, we found that the volume expansibility of microgels was much larger than that of the bulk MR gel (quantitative data not shown), indicating that the enlarged size and residual anisotropy of microgels are mainly caused by the internal fracture of microgels, rather than by the permanent deformation of the outer matrix phase. Thus, the enlarged size and residual anisotropy of microgels give the convincing evidence that microgels structure was broken and they serve as sacrificial bonds to reinforce MR gels, in consistent with the result from macroscopic elongation. Furthermore, the microgels in the reswollen gel still kept their integrity and did not break into pieces, which disproves the assumption of that the rigid network in DN gels was fractured into independent micro-"clusters" after being stretched proposed in the previous research.[35] Considering the embedded microgels as probe during or after elongation, we have obtained some valuable results in mesoscale to study the fracture mechanism on these novel MR gels. These results also demonstrate that studying on the mesoscale fracture of microgels will bridge the gap between macroscopic mechanical properties and microscopic structure change.

From the DN reinforcement principle, it is expectable that MR gels from polyelectrolyte microgels would show high mechanical strength and toughness. However, MR gel from neutral microgels also achieved the comparable high strength and toughness, which is impossible for the conventional bulk DN gels. This is probably explained that the neutral PAAm microgels interpenetrated by the first polymerized PAAm network will be swollen much under the additional osmotic pressure of the PAAm network, close to the swelling ratio of polyelectrolyte microgels, so can be reinforced effectively by the second polymerized PAAm network. So far, it is the only hydrogel with high strength and toughness from only one chemical component, by skillfully combining the dense PAAm microgel with the dilute PAAm matrix. Taking advantage of its high transparency and weak-adhesive nature to cells,[37] this MR(0) gel might be a more superior candidate as a kind of wound dressing than other polyelectrolyte MR gels. The development of wound healing could be monitored in real time, even if the wound is covered by a sheet of MR(0) gel.

To some extent, MR gels show the similar structure with carbon black (CB) reinforced rubbers, and both of them are reinforced by adding the rigid fillers, which effectively reduce stress concentration through the spatial self-adjustment of fillers or chains. However, the essential differences are summarized as follows: (1) The desorption between CB and the matrix is prevented in CB-reinforced rubbers only when the fillers' size is below about 50 nm,[38] due to the low surface energy of CB that decreases with the increase in size, but in MR gels, the microgels with diameters of ca. 5 μm still effectively improve the mechanical strength. (2) The bonding between CB fillers and the rubber matrix is attributed to the interfacial physical adsorption and chemical adsorption, but the bonding in MR gels is attributed to the interpenetration between the microgels and the neutral network. (3) The internal fracture of CB-reinforced rubbers stems from the failure in the interfacial layer, while that of MR gels arises from the rupture of covalent bonds inside the microgels. MR hydrogels composed of DN microgels, with the innovative two-phase composite structure, have shown the unique structure and reinforcement mechanism. If this structure and reinforcement mechanism of MR hydrogel is expanded to the field of rubber, one might expect more improved mechanical strength than the traditional CB-reinforced rubbers.

■ CONCLUSIONS

Strong and tough hydrogels with the novel two-phase composite structure, MR hydrogels, have been prepared by salt-controlled swelling of various quasi-monodisperse microgels and two-step sequential UV polymerization of neutral PAAm networks and show the comparable mechanical strength with the conventional bicontinuous DN hydrogels. The microgels embedded in the MR hydrogel films are considered as DN microgels, serving as probe to visualize the mesoscale fracture process during and after tensile test by optical microscope. We have a preliminary idea that the high mechanical strength and toughness of MR gels roots in the sacrificial bonds of the microgels that fracture during deformation. The reinforcement mechanism based on microgels incorporation has the universality for various microgels with the different charges. The successful design of MR gels helps us to understand DN hydrogels more profoundly. We have found that whether the first network is polyelectrolyte or continuous phase or not is not significant. The reinforcement mechanism of MR gels is promising not only for gel science but also for the field of rubber. Furthermore, the tunable microgels in the tough MR gels, such as encapsulation of drugs or silver, will meet extensive requirements as wound dressings. The tough and large extensible nature of the MR gel films will greatly merit the use of hydrogels as an extracellular matrix for the mechanical stress-directed differentiation of embryonic stem (ES) cells or induced-pluripotent stem (iPS) cells.[39]

■ AUTHOR INFORMATION

Corresponding Author

*E-mail: gong@mail.sci.hokudai.ac.jp.

■ ACKNOWLEDGMENT

This research was financially supported by a Grant-in-Aid for Specially Promoted Research (No. 18002002) from the Ministry of Education, Science, Sports and Culture of Japan.

■ REFERENCES

(1) Peppas, N. A.; Hilt, J. Z.; Khademhosseini, A.; Langer, R. *Adv. Mater.* **2006**, *18*, 1345.
(2) Calvert, P. *Adv. Mater.* **2009**, *21*, 743.
(3) Gong, J. P.; Katsuyama, Y.; Kurokawa, T.; Osada, Y. *Adv. Mater.* **2003**, *15*, 1155.
(4) Myung, D.; Koh, W. U.; Ko, J. M.; Hu, Y.; Carrasco, M.; Noolandi, J.; Ta, C. N.; Frank, C. W. *Polymer* **2007**, *48*, 5376.
(5) Myung, D.; Waters, D.; Wiseman, M.; Duhamel, P. E.; Noolandi, J.; Ta, C. N.; Frank, C. W. *Polym. Adv. Technol.* **2008**, *19*, 647.
(6) Waters, D. J.; Engberg, K.; Parke-Houben, R.; Hartmann, L.; Ta, C. N.; Toney, M. F.; Frank, C. W. *Macromolecules* **2010**, *43*, 6861.
(7) Okumura, Y.; Ito, K. *Adv. Mater.* **2001**, *13*, 485.
(8) Haraguchi, K.; Takehisa, T. *Adv. Mater.* **2002**, *14*, 1120.
(9) Haraguchi, K.; Li, H. J. *Angew. Chem., Int. Ed.* **2005**, *44*, 6500.
(10) Haraguchi, K.; Li, H. J. *Macromolecules* **2006**, *39*, 1898.
(11) Shin, M. K.; Spinks, G. M.; Shin, S. R.; Kim, S. I.; Kim, S. J. *Adv. Mater.* **2009**, *21*, 1712.
(12) Sakai, T.; Matsunaga, T.; Yamamoto, Y.; Ito, C.; Yoshida, R.; Suzuki, S.; Sasaki, N.; Shibayama, M. *Macromolecules* **2008**, *41*, 5379.
(13) Wang, Q.; Mynar, J.; Yoshida, M.; LEE, E.; LEE, M.; Okuro, K.; Kinbara, K.; Aida, T. *Nature* **2010**, *463*, 339.
(14) Kaneko, T.; Tanaka, S.; Ogura, A.; Akashi, M. *Macromolecules* **2005**, *38*, 4861.
(15) Henderson, K. J.; Zhou, T. C.; Otim, K. J.; Shull, K. R. *Macromolecules* **2010**, *43*, 6193.
(16) Zhang, K.; Lackey, M. A.; Cui, J.; Tew, G. N. *J. Am. Chem. Soc.* **2011**, *133*, 4140.
(17) Tang, L.; Liu, W. G.; Liu, G. P. *Adv. Mater.* **2010**, *22*, 2652.
(18) Haque, M. A.; Kamita, G.; Kurokawa, T.; Tsujii, K.; Gong, J. P. *Adv. Mater.* **2010**, *22*, 5110.
(19) Zhang, X. Z.; Chu, C. C. *Polymer* **2005**, *46*, 9664.
(20) Cho, E. C.; Kim, J. W.; Nieves, A. F.; Weitz, D. A. *Nano Lett.* **2008**, *8*, 168.
(21) Sahiner, N.; Singh, M. *Polymer* **2007**, *48*, 2827.
(22) Lin, W. C.; Fan, W.; Marcellan, A.; Hourdet, D.; Creton, C. *Macromolecules* **2010**, *43*, 2554.
(23) Huang, T.; Xu, H. G.; Jiao, K. X.; Zhu, L. P.; Brown, H. R.; Wang, H. L. *Adv. Mater.* **2007**, *19*, 1622.
(24) Yu, Q. M.; Tanaka, Y.; Furukawa, H.; Kurokawa, T.; Gong, J. P. *Macromolecules* **2009**, *42*, 3852.
(25) Saito, J.; Furukawa, H.; Kurokawa, T.; Kuwabara, R.; Kuroda, S.; Hu, J.; Tanaka, Y.; Gong, J. P.; Kitamura, N.; Yasuda, K. *Polym. Chem.* **2011**, *2*, 575.
(26) Cheng, C. J.; Chu, L. Y.; Zhang, J.; Wang, H. D.; Wei, G. *Colloid Polym. Sci.* **2008**, *286*, 571.
(27) Nisisako, T. *Chem. Eng. Technol.* **2008**, *31*, 1091.
(28) Liang, S.; Yu, Q. M.; Yin, H.; Wu, Z. L.; Kurokawa, T.; Gong, J. P. *Chem. Commun.* **2009**, 7518.
(29) Pook, L. P.; Sharples, J. K. *Int. J. Fract.* **1979**, *15*, 223.
(30) Greensmith, H. W.; Thomas, A. G. *J. Polym. Sci.* **1955**, *18*, 189.
(31) Furukawa, H.; Kuwabara, R.; Tanaka, Y.; Kurokawa, T.; Na, Y.-H.; Osada, Y.; Gong, J. P. *Macromolecules* **2008**, *48*, 7173.
(32) Nakajima, T.; Furukawa, H.; Tanaka, Y.; Kurokawa, T.; Osada, Y.; Gong, J. P. *Macromolecules* **2009**, *42*, 2184.
(33) Greensmith, H. W. *J. Polym. Sci.* **1960**, *3*, 175.
(34) Gong, J. P. *Soft Matter* **2010**, *6*, 2583.
(35) Na, Y.-H.; Tanaka, Y.; Kawauchi, Y.; Furukawa, H.; Sumiyoshi, T.; Gong, J. P.; Osada, Y. *Macromolecules* **2006**, *39*, 4641.
(36) Liang, S. M.; Wu, Z. L.; Hu, J.; Kurokawa, T.; Yu, Q. M.; Gong, J. P. *Macromolecules* **2011**, *44*, 3016.
(37) Chen, Y. M.; Yang, J. J.; Gong, J. P. *J. Adhes.* **2009**, *85*, 830.
(38) Edwards, D. C. *J. Mater. Sci.* **1990**, *25*, 4175.
(39) Cushing, M. C.; Anseth, K. S. *Science* **2007**, *316*, 1133.